Euromech Colloquium n. 541
New Advances in the Nonlinear Dynamics and Control of Composites for Smart Engineering Design
Senigallia, Italy, June 3-6, 2013

A new computational method for nonlinear normal modes of nonconservative systems

L. Renson, G. Kerschen
Aerospace and Mechanical Engineering Department, University of Liège, Belgium.
l.renson@ulg.ac.be, g.kerschen@ulg.ac.be

Abstract. The concept of nonlinear normal modes (NNMs) was introduced with the aim of providing a rigorous generalization of normal modes to nonlinear systems. Initially, NNMs were defined as periodic solutions of the underlying conservative system, and continuation algorithms were recently exploited to compute them. To extend the concept of NNMs to nonconservative systems, Shaw and Pierre defined an NNM as a two-dimensional invariant manifold in the system's phase space.
This contribution presents a novel algorithm for solving the set of partial differential equations governing the manifold geometry numerically. The resolution strategy takes advantage of the hyperbolic nature of the equations to progressively solve them in annular regions. Each region is defined by two different iso-energy curves and equations are discretized using a specific finite element technique. The proposed strategy also offers the opportunity to estimate the frequency-energy dependence of the mode without using time integration. The algorithm is applied to both conservative and nonconservative systems.

1. INTRODUCTION

Pioneered in the 1960s by Rosenberg [1, 2], NNMs were defined as a *vibration in unison* of a nonlinear system. Later extended to embrace all periodic solutions [3], this definition leads to efficient and versatile computational methods for NNMs (see, e.g., [4, 5]) that are, however, a priori limited to conservative systems. Shaw and Pierre proposed a generalization of Rosenberg's definition that provides an elegant extension of NNMs to damped systems. Based on geometric arguments and inspired by the center manifold theory, they defined an NNM as a two-dimensional invariant manifold in phase space [6].

The first attempt to carry out numerical computation of NNMs as invariant manifolds is that of Pesheck et al. [7]. The manifold-governing partial differential equations (PDEs) are solved in modal space using a Galerkin projection with the NNM motion parameterized by amplitude and phase variables. The approach developed in [7] uses global shape functions to discretize the NNM PDEs, i.e. shape functions defined over the entire computational domain. The discretization ends up with a set of highly-coupled and highly-nonlinear algebraic equations to solve. As a consequence, the computational burden was dramatically increased as the number of degrees of freedom of the mechanical system increases and a "shift in tactics" was needed [7]. A semi-discrete approach was then introduced by dividing the amplitude domain into several sub-domains in order to reduce the complexity of the shape functions in amplitude.

Another interesting approach uses a Fourier-Galerkin procedure to solve a nonlinear eigenvalue problem with NNMs defined in terms of a frequency and a modal vector both

functions of amplitude and phase. First established for conservative systems [8], this method was then extended to nonconservative ones [9]. Despite the interesting presence of a series expansion whose coefficients can provide valuable insight into the dynamics, the method suffers from a dramatically increasing computational burden as the number of DOFs increases. Indeed, yet different, [7] and [9] share a similar discretization strategy to solve NNMs.

In [10], NNMs are viewed as complex modes. An eigenvalue problem in terms of these complex modes and generalized Fourier series is defined. The method extends classical continuation approaches to nonconservative systems. Alike [6], this approach issues from the observation that LNMs can be viewed as complex quantities in the presence of damping. This complex character accounts for the phase lag between the different DOFs of the system. In [6], they further showed that this complex formulation is similar to a displacement-velocity description of the mode which in turn was extended to NNMs.

In a recent contribution, Touzé and co-workers [11] also tackled the PDEs in modal space. They show that these PDEs can be interpreted as a transport equation, which, in turn, can be discretized using finite differences. Their method revealed accurate for conservative systems but not yet applicable to nonconservative ones.

The present study introduces a new method for the computation of NNMs defined as invariant manifolds in phase space. The transformation of the manifold-governing PDEs to modal space is not necessary, which means that an NNM motion is parametrized by master displacement and velocity, as in [12].

Targeting the computation of NNMs for high-dimensional systems such as those encountered in industry, we propose to solve the set of PDEs using the finite element method (FEM), which employs local shape functions. The FEM renders the algorithm general and systematic. The computation of the dynamics reduced on the manifold relies directly on the finite element interpolation and no additional interpolation is needed (unlike, e.g., with finite differences [11]). In addition, we underline the specific treatment required by the type of equations governing the NNMs. The proposed algorithm is particularly adapted to these equations.

The present paper is organized as follows. Theoretical concepts about NNMs defined as invariant manifolds are briefly introduced in Section 2. Section 3 details the proposed algorithm. The FEM is presented as well as our specific treatment of boundary conditions. The method to estimate the motion frequency is presented in Section 4. In Section 5, our algorithm is validated on a 2DOF system composed of quadratic and cubic nonlinearities. The validation procedure involves comparison with an algorithm for the continuation of periodic solutions. Along this example, the novel strategy to recover an estimation of the motion frequency is validated. Linear damping is then introduced into the system and the applicability of the algorithm is demonstrated. Finally, in Section 6, an example with two coupled Van der Pol oscillators is considered. Accurate results are obtained on this nonlinearly damped system.

2. MANIFOLD GOVERNING PDES

A detailed description of NNMs and of their fundamental properties (e.g., frequency-energy dependence, bifurcations, and stability) is given in [3, 13] and is beyond the scope of this paper.

In the present contribution, the free response of discrete mechanical systems with N degrees of freedom (DOFs) is considered, assuming that continuous systems (e.g., beams, shells, or plates) have been spatially discretized using the FE method. The equations of motion are

$$\mathbf{M}\ddot{\mathbf{x}}(\mathrm{t}) + \mathbf{C}\dot{\mathbf{x}}(\mathrm{t}) + \mathbf{K}\mathbf{x}(\mathrm{t}) + \mathbf{f}_{\mathrm{nl}}\{\mathbf{x}(\mathrm{t}), \dot{\mathbf{x}}(\mathrm{t})\} = 0 \tag{1}$$

where **M**, **C**, and **K** are the mass, damping, and stiffness matrices, respectively; **x**, $\dot{\mathbf{x}}$, $\ddot{\mathbf{x}}$ are the displacement, velocity, and acceleration vectors, respectively; $\mathbf{f}_{nl}$ is the nonlinear restoring force vector.
To provide a rigorous definition of the NNM concept to damped systems, Shaw and Pierre defined an NNM as a two-dimensional invariant manifold in phase space [6]. In order to parametrize the manifold, a single pair of state variables (i.e., both the displacement and the velocity) are chosen as master coordinates, the remaining variables being functionally related to the chosen pair (eq. (2)).

$$\begin{cases} x_i = X_i(u, v), \\ y_i = Y_i(u, v), \end{cases} \qquad i = 1, \dots, N; i \neq k \tag{2}$$

Using a similar approach as for the center manifold technique, the time dependence in the equations is eliminated and leads to a set of $2N - 2$ partial differential equations (PDEs) that can be solved for the X_i's and Y_i's:

$$\begin{cases} Y_i = \frac{\partial X_i}{\partial u} v + \frac{\partial X_i}{\partial v} f_k(u, \boldsymbol{X}, v, \boldsymbol{Y}), \\ f_i = \frac{\partial Y_i}{\partial u} v + \frac{\partial Y_i}{\partial v} f_k(u, \boldsymbol{X}, v, \boldsymbol{Y}), \end{cases} \qquad i = 1, \dots, N; i \neq k \tag{3}$$

where $\boldsymbol{X} = \{X_j : j = 1, \dots, N; j \neq k\}$, $\boldsymbol{Y} = \{Y_j : j = 1, \dots, N; j \neq k\}$, and f_j accounts for all the forcing terms in the equations (linear/nonlinear stiffness and damping). Equations for $i = k$ are trivially satisfied. Once the manifold-governing PDEs are solved, constraint equations (2) represent the geometrical description of the NNM. Around the equilibrium point, eqs. (3) admit N solutions, i.e., one for each mode. Geometrically, LNMs are represented by planes in phase space, and NNMs are two-dimensional surfaces that are tangent to them at the equilibrium point. The curvature of the NNM surface is purely due to nonlinear effects.

3. FINITE ELEMENT COMPUTATION OF NNMS

To fit into a formulation more convenient to the FEM, eqs. (3) are recast into eqs. (4) where $\boldsymbol{\nabla}$ is the gradient vector and $\boldsymbol{V}^T = \{v\ f_k\}$. Targeting a solution for finite amplitudes, equations are solved in a domain Ω whose boundary is $\partial\Omega$. This boundary comprises an inflow boundary $\partial\Omega^- = \{\boldsymbol{u} = (u, v) \in \partial\Omega : \boldsymbol{V}(\boldsymbol{u}).\boldsymbol{n}(\boldsymbol{u}) < 0\}$ and an outflow $\partial\Omega^+ = \{\boldsymbol{u} = (u, v) \in \partial\Omega : \boldsymbol{V}(\boldsymbol{u}).\boldsymbol{n}(\boldsymbol{u}) > 0\}$. $\boldsymbol{n}(\boldsymbol{u})$ is the outward normal vector to $\partial\Omega$. The $2N - 2$ equations are quasilinear first-order hyperbolic partial differential

equations that are similar to flow equations encountered in fluid dynamics. This interpretation of the PDEs is identical to the interpretation made by Touzé and its co-workers [11] who interpreted the PDEs as a transport problem. The vector $\boldsymbol{V}$ can therefore be interpreted as the velocity vector of the master coordinates flow. The flow direction is called the characteristic direction and illustrates the propagation of the information into the domain.

$$\begin{cases} \boldsymbol{V}.\boldsymbol{\nabla} X_i - Y_i = 0 \\ \boldsymbol{V}.\boldsymbol{\nabla} Y_i - f_i = 0 \\ X_i|_{\partial\Omega^-} = X_i^- \\ Y_i|_{\partial\Omega^-} = Y_i^- \end{cases} \qquad i = 1, \dots, N; i \neq k, \boldsymbol{V}^T = \{v\ f_k\} \tag{4}$$

Figure 1(a) shows the flow of a 2DOF nonlinear conservative system. In the domain Ω, characteristic directions form curves called characteristic curves (or characteristics). In the present case, the conservation of the energy induces closed characteristics and results in a clear distinction between the dynamics of different energies. Indeed, the "information" related to a given energy is limited to the corresponding characteristic. This illustrates there is no mixing between different energy dynamics; high and low energy dynamics do not influence each other. In the non-conservative case, characteristics spiral toward the equilibrium point of the system (here, the origin) (see Figure 1(b)).

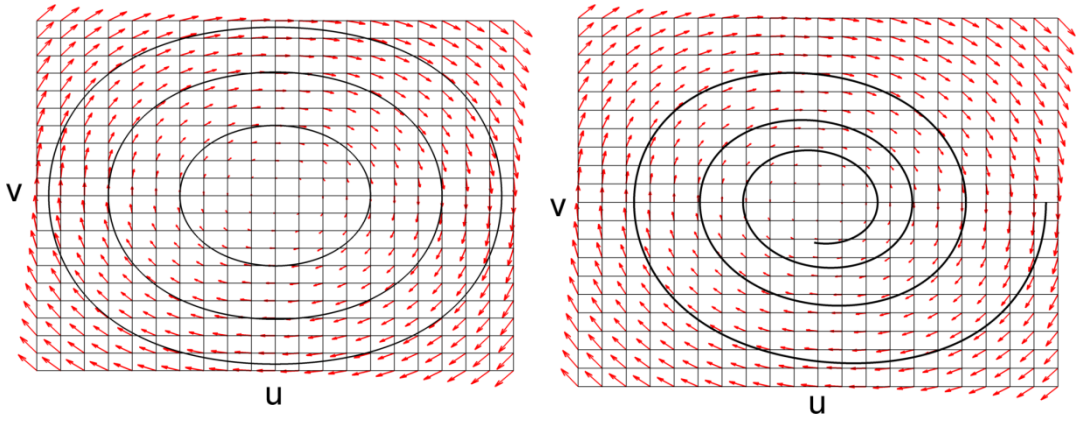

Figure 1. PDEs are interpreted as flow equations where $\boldsymbol{V}$ is the velocity field (→). (a) For a conservative system, the flow is tangent to iso-energy curves. (b) For a nonconservative system, the flow spirals to the equilibrium point.

Solving hyperbolic PDEs requires boundary conditions at inflow ($\partial\Omega^-$), i.e. where the velocity vector $\boldsymbol{V}$ points inward the domain (cf. also [11]). In our first order problem, it requires to set the unknown field values (X_i^-, Y_i^-) on this boundary. However, the domain boundary is away from the equilibrium point and corresponds to a region of high-energy where no theoretical information about the manifold is available. A first (classical) strategy would be to use an extrapolation technique to estimate the unknown values at the boundary using the solution computed inside the domain. According to the above interpretation in terms of characteristics, this will involve a mixing between different energy dynamics. Extrapolation was therefore not deemed useful. Nevertheless, we note that a domain with an iso-energy curve for boundary remains everywhere tangent to the flow and boundary conditions become theoretically obsolete. Assuming two different iso-energy curves, they form the inner and outer boundaries of an annular domain. Since a clear partition of the dynamics exists, one can solve the PDEs in this region disregarding

the solution computed outside it. This strategy is key to our algorithm. It avoids setting disruptive boundary conditions and reduces the computational burden. This is particularly interesting as the number of degrees of freedom of the mechanical system becomes large.

For nonconservative systems, there is no partition of the dynamics and the flow points inward the domain boundary. However, the methodology suggested previously remains applicable. Indeed, let's take an annular domain whose inner and outer boundaries correspond to iso-energy curves. Generally speaking, the flow points in and out at the outer and inner boundaries; respectively. However, mathematically, an "inverse" problem where boundary conditions have to be specified at the inner boundary can be solved. The flow can be "inverted" and spiral in and out at the inner and outer boundary; respectively. A recursive strategy can then be applied to progressively solve the PDEs using the previously computed solution as boundary conditions for the next domain.

The proposed strategy suffers from a single limitation that is: iso-energy curves are only known at the solution. To circumvent this issue, a first guess of the iso-energy curve is computed using the previous domain boundary and solution. Then the shape of the new computational domain is iteratively modified as the new solution is computed. At the solution, the domain boundary fits the actual iso-energy curve.

3.1 Resolution Strategy Overview

The resolution strategy is illustrated in Figure 2. The computation starts in a small domain around the origin where the system is assumed to behave linearly. The domain boundary is established for a given initial energy and computed using the dynamics of a LNM. The LNM selected corresponds to the targeted NNM. The LNM is also considered as a first guess for the solution. To compute the actual solution, the domain boundary is corrected in order to fit the iso-energy corresponding to the current estimation of the solution. The correction is performed thanks to a mesh moving technique. It is applied a user-defined number of times until some criteria are fulfilled. Domain corrections precede each correction of the PDE solution in order to satisfy the boundary conditions. Once the solution is computed within a given accuracy, a new annular domain can be predicted. The prediction of the next iso-energy is performed using the previously computed solution. The new curve is considered as the new outer boundary whereas the old outer boundary becomes the inner one. Both boundaries define the new computational domain. The solution on this new annular region can be computed following a similar sequence of domain-correction and solution-correction. The NNM computation stops when the manifold is folded such that it cannot be described in terms of a single pair of master coordinates (e.g., during modal interactions). Post-processing is performed in order to merge the different annular domains computed. This operation is a simple "global" mesh interpolation over all "local" meshes.

We here stress the importance of the iterative approach in annular regions. It first comes from the need to impose boundary conditions close to the origin for nonconservative systems (where the manifold is "known"). This strategy reveals particularly interesting in "complicated" problems where the initial LNM is too far from the actual manifold. Finally, in the presence of numerous DOFs, it dramatically reduces the computational burden.

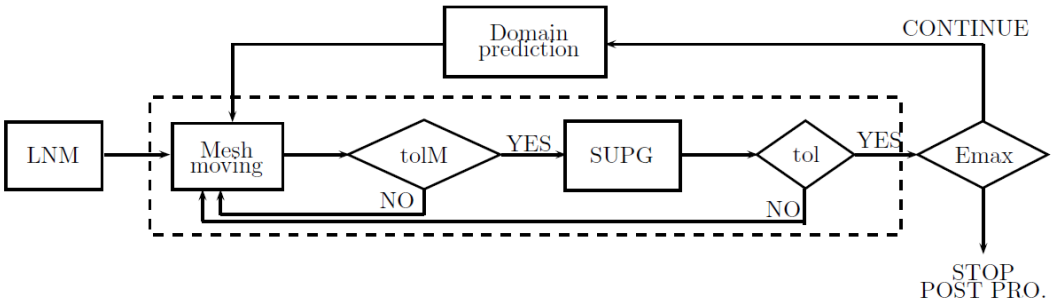

Figure 2. Schematics of the alogirthm resolution strategy.

3.2 Streamline Upwind Petrov-Galerkin

In order to solve hyperbolic PDEs using the FEM, specific numerical techniques are employed. Indeed, classical Galerkin finite element formulations using similar shape and test function spaces have demonstrated poor results, for instance, in the context of fluid dynamics [14, 15]. In a similar way to off-centred schemes in the finite difference framework, several finite element formulations deal with transport phenomena using alternative test functions. The SUPG method is used herein and consists in over-weighting the shape functions that are upstream. This method falls within the general category of Petrov-Galerkin formulations where test and shape functions are taken in different spaces. The approach is rather standard and its description is out of the scope of our paper. We briefly present the major points of our formulation and the interested reader can refer to [15] for practical details about SUPG.

To derive our finite element formulation, a weighted residual approach is applied to eqs. (4). The formulation is presented in eqs. (5) where $i = 1, \dots, N$ with $i \neq k$ and where shape functions are considered as simple first-order Lagrange shape functions: $N^b \in P^1$. The test functions are $\widetilde{N}^b = N^b + \tau \boldsymbol{V}.\boldsymbol{\nabla} N^b$. As already mentioned, test functions differ from classical Galerkin test functions via an upstream overweighting ($\tau \boldsymbol{V}.\boldsymbol{\nabla} N^b$). As a consequence, discontinuous test functions are employed [16].

$$\begin{aligned} &\iint_\Omega \left[V(u,X,v,Y).\nabla X_i(u,v) - Y_i(u,v)\right] \delta\widetilde{Y}_i \, du \, dv = 0 \\ &\iint_\Omega \left[V(u,X,v,Y).\nabla Y_i(u,v) - f_i(u,v)\right] \delta\widetilde{X}_i \, du \, dv = 0 \end{aligned} \tag{5}$$

The parameter τ can be defined according to various definitions [17-20]. Here, $\tau = \frac{h^e}{2\|V\|_2}$ and h^e is the characteristic size of mesh elements.

After the FE discretization, the set of PDEs is transformed to a set of coupled nonlinear algebraic equations. These equations are solved using a Newton-Raphson procedure where the Jacobian matrix is provided analytically. Each iteration involves the solution of a large linear system. It is computed using the GMRes ("Generalized Minimal Residual") iterative solver and left and right ILU preconditioners ("Incomplete LU"). An important feature of our problem is that equations to solve remains nonlinear even if the mechanical system considered is linear.

3.3 Domain Prediction

The prediction of the domain $d+1$ is performed using an approach similar to continuation. Consider the outer boundary E^d. This outer boundary becomes the inner boundary of the next domain $d+1$. To compute the new outer boundary, an energy increment ΔE^d is applied and an estimation of the iso-energy curve at $E^{d+1} = E^d + \Delta E^d$ is determined. Linearizing the energy around each point i of the boundary d and solving eq. (6) transforms energy increments in terms of displacements $(\Delta u_i, \Delta v_i)$ to apply to boundary nodes. Figure 3 illustrates the result of this procedure.

$$\Delta E^d = \left.\frac{dE}{du}\right|_i^d \Delta u_i + \left.\frac{dE}{dv}\right|_i^d \Delta v_i, \qquad \forall i \tag{6}$$

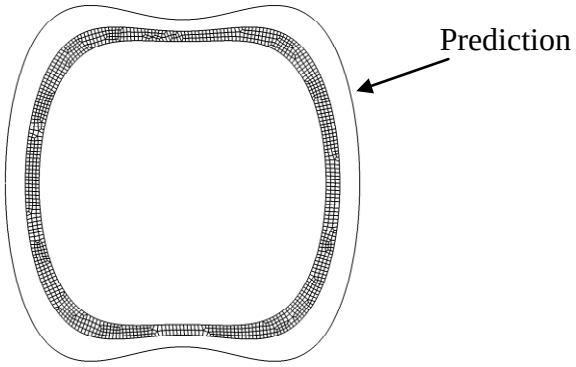

Figure 3. Prediction of the next domain boundary using the last converged solution.

3.4 Domain Correction using a Mesh Moving Technique

As introduced, the shape of the computational domain is chosen in order to avoid imposing boundary conditions. Such a domain needs to be everywhere tangent to the flow $\boldsymbol{V}$. In the particular case of a conservative system, the flow is everywhere tangent to iso-energy curves. An iso-energetic domain boundary would therefore meet our requirement. Unfortunately, such curves are known at the solution and only a prediction of it can be performed. In order to satisfy the need of boundary conditions to solve the hyperbolic problem, the domain is modified at each iteration such that it is an iso-energy curve for the current estimation of the solution. At each iteration, BCs are thus satisfied and the hyperbolic problem is well posed.

To modify the domain's shape, the mesh is considered as a pseudo-elastic medium and a linear elasticity problem is solved. The inner boundary is considered as clamped (displacements are set to zero) while the outer boundary is moved in order to equal a reference energy. This reference energy is considered to be the smallest energy of all boundary points. This choice has the advantage to consider a new boundary completely enclosed into the previous one. The data interpolation between both meshes is therefore obvious and does not require any extrapolation. The formula used to compute the displacements imposed to the boundary nodes are similar to formula used for domain prediction (cf. Eq. (6)). The only difference is the energy increment ΔE that is now determined to equal the reference energy. Additional information about mesh moving techniques can be found in [21].

4. FREQUENCY COMPUTATION

A key step in the derivation of the PDEs governing the manifold is the removal of the time dependence of the equations. As a consequence, time does not appear anymore in the equations and NNMs are geometrically described with PDEs. Therefore, contrary to methods using the system's ODEs where explicit time dependence is present, the invariant manifold approach does not provide a straightforward access to the motion frequency.

However, in the restrictive case of conservative systems, "post-processing" operations can be applied in order to combine standard continuation techniques on the reduced-dynamic ODEs. In the present study, we developed a novel approach to estimate the motion frequency as a byproduct of our finite element strategy. This approach is based on the interpretation of PDEs as hyperbolic equations and on the "iso-energetic" resolution strategy we employ. It does not rely on the reduced-dynamic ODEs, so time integration and continuation are not needed.

PDEs are solved in the Ω, i.e. (u, v) plane where each domain boundary corresponds to an iso-energy curve. If the reduced dynamics was integrated with initial conditions on one of these curves, all the points belonging to the time series would geometrically lie on a domain boundary. Therefore the points describing the contour of the finite element mesh also belong to this time series and the contour corresponds to one period of motion. In order to compute the motion frequency, the contour length is divided by the averaged norm of the velocity $\boldsymbol{V}$ along each edge. As evidenced in Section 5, a very good agreement with reference results is achieved.

For conservative systems, this method efficiently replaces a continuation algorithm but its extension to nonconservative problems is left for future work.

5. A GEOMETRICALLY NONLINEAR 2DOF SYSTEM

In this section, we first demonstrate the applicability of our method on a conservative two-degree-of-freedom system governed by Equations (7). This system was first presented in [8, 11, 22]. In [22], the authors showed the importance of NNMs for dynamical analysis and reduced-order modelling. The influence of linear damping was also evidenced as it could turn a hardening system to softening behaviour. In the present paper, we also consider this 2DOF system as a benchmark. Our finite element method will be validated in both conservative and nonconservative cases.

$$\begin{aligned} &\ddot{X}_1 + 2\omega_1\xi_1\dot{X}_1 + \omega_1^2 X_1 + \frac{\omega_1^2}{2}(3X_1^2 + X_2^2) + \omega_2^2 X_1 X_2 + \frac{\omega_1^2+\omega_2^2}{2} X_1(X_1^2 + X_2^2) = 0 \\ &\ddot{X}_2 + 2\omega_2\xi_2\dot{X}_2 + \omega_2^2 X_2 + \frac{\omega_2^2}{2}(3X_2^2 + X_1^2) + \omega_1^2 X_1 X_2 + \frac{\omega_1^2+\omega_2^2}{2} X_2(X_1^2 + X_2^2) = 0 \end{aligned} \quad (7)$$

System's nonlinearities arise from second order terms in the stress tensor. Due to the geometrical configuration, equations are naturally uncoupled at the linear stage. As illustrated in [23] the hardening and softening behaviour of the conservative system is fully determined with ω_1 and ω_2; the linear parameters. We first consider the conservative case where the linear modal damping parameters from eqs. (7), ξ_1 and ξ_2, equal zero.

Figure 4(a-b) present the two-dimensional invariant manifold with both X_2 and Y_2 slave coordinates for the first NNM. $\omega_1^2 = 1$ and $\omega_2^2 = 3$. The solution of our finite element method is depicted in green. For this conservative system, a reference solution coming from a continuation of periodic solutions algorithm [5] is presented in yellow. A very good agreement between both surfaces is observed. In Figure 4(c), the frequency dependence of the first NNM versus energy is presented in a frequency-energy plot (FEP). The black line is the reference solution from the continuation algorithm. Full and dashed parts illustrate the stable and unstable character of the periodic solutions. The computation of the frequency using the different domain boundaries is presented with blue markers. We observe a softening effect in perfect agreement with the reference. The frequency-energy discretization is linked to the energy steps performed by the algorithm computing for the invariant manifold.

We now consider the second NNM. Likewise the first NNM, the geometry of the invariant manifold perfectly matches the reference solution and the FEP is well reproduced (Figure 5(a)). To further evidence these accurate results, Figure 5(b) compares the dynamics reduced on the invariant manifold (in black) with respect to the full-system dynamics (in red). The excellent correspondence between both slave velocity time series demonstrates the accurate computation of the invariant manifold. As already mentioned, the computation of the dynamics is based on the finite element interpolation mesh and does not require any additional interpolation procedure. It results in an efficiently and accurately computed dynamics that perfectly reflects the accuracy of the method on the invariant manifold.

We finally note the computation of the manifold for unstable regimes. In these unstable regions, a small error performed on the computation of the manifold results in an error on initial conditions that are no more in the invariant manifold and the "true dynamics" drifts apart from the reduced one. Figure 5(c) shows Y_1 for larger initial conditions. Over 8 periods, both dynamics accurately match. Then, as the small error on initial conditions gets bigger, the true dynamics rapidly branches off the reduced one. As a consequence, accurate time integration over multiple periods requires a finer mesh compared to stable regions. The investigation of the NNMs stability is not considered in the present paper.

A further validation of our frequency computation is presented in Figure 6 with $(\omega_1^2, \omega_2^2) = (1.7,6)$. The hardening behaviour of the system rapidly turns to softening. This is a characteristic phenomenon of geometrically nonlinear systems involving quadratic and cubic stiffnesses [22, 23]. Here it is well reproduced by our method.

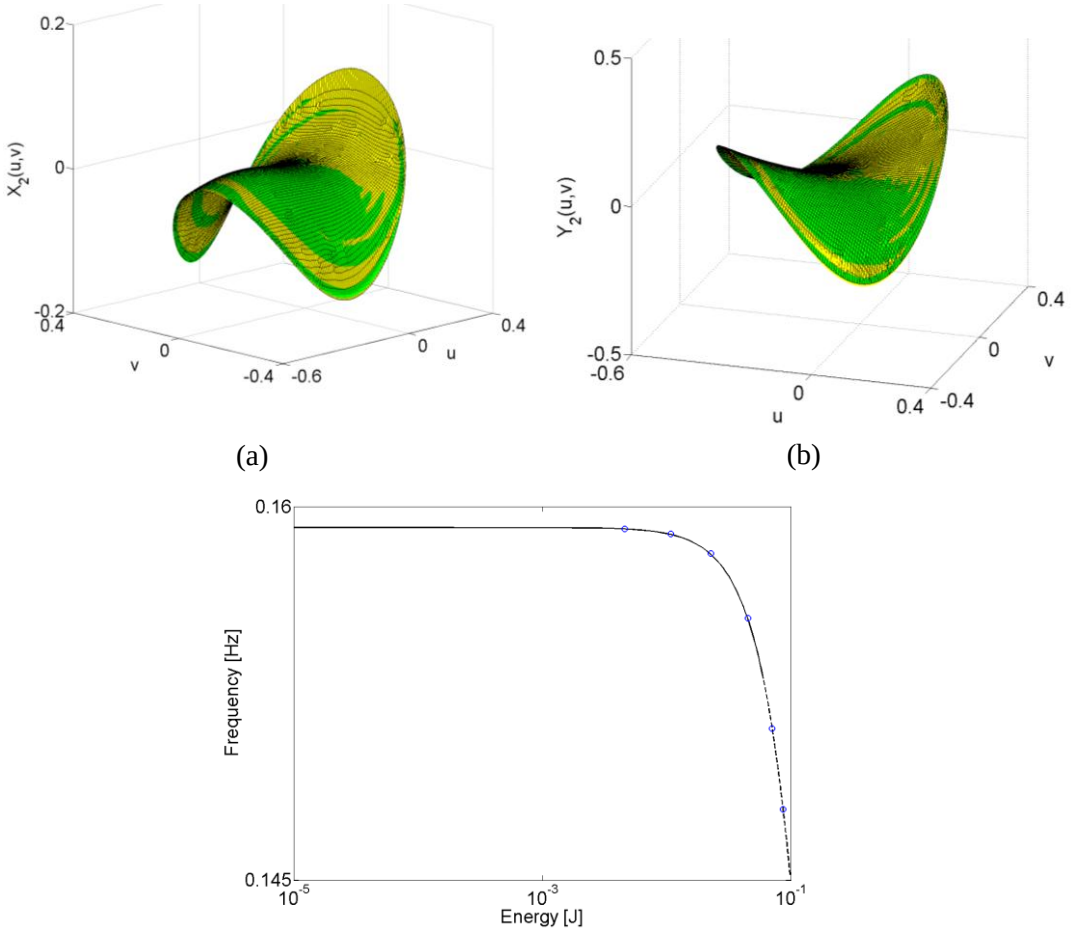

Figure 4. First NNM. (a,b) Slave displacement $\boldsymbol{X_2}$ and valocity $\boldsymbol{Y_2}$ (in green) are compared to reference results from a continuation of periodic solutions algorithm (in yellow). Very good agreement is observed. (c) Comparison between the frequencies extracted from the invariant manifold (O) and the reference FEP from continuation. The dashed line corresponds to the unstable part of the backbone.

We now turn to the analysis of the system including linear damping ($(\xi_1, \xi_2) \neq 0$). We specifically consider the case where $(\omega_1^2, \omega_2^2) = (1.8,6)$. In Figure 7, the system forced response is computed for different excitation amplitudes. For increasing values of the damping ratio ξ_2, i.e. from Figure 7(a) to Figure 7(b), the hardening behaviour of the system is modified into softening.

Computing the invariant manifold for both system parameters offers a way to observe this frequency dependence. In this nonconservative case, the reduced dynamics is integrated versus time and a time-frequency analysis is performed using the wavelet transform. For both systems (Figure 7(a-b)), the NNM backbone is depicted with a dash-dot line. The steps that appear result from the time-frequency resolution of the transformation. In spite of this time-frequency resolution compromise, NNMs backbones reproduce the system resonances under harmonic forcing.

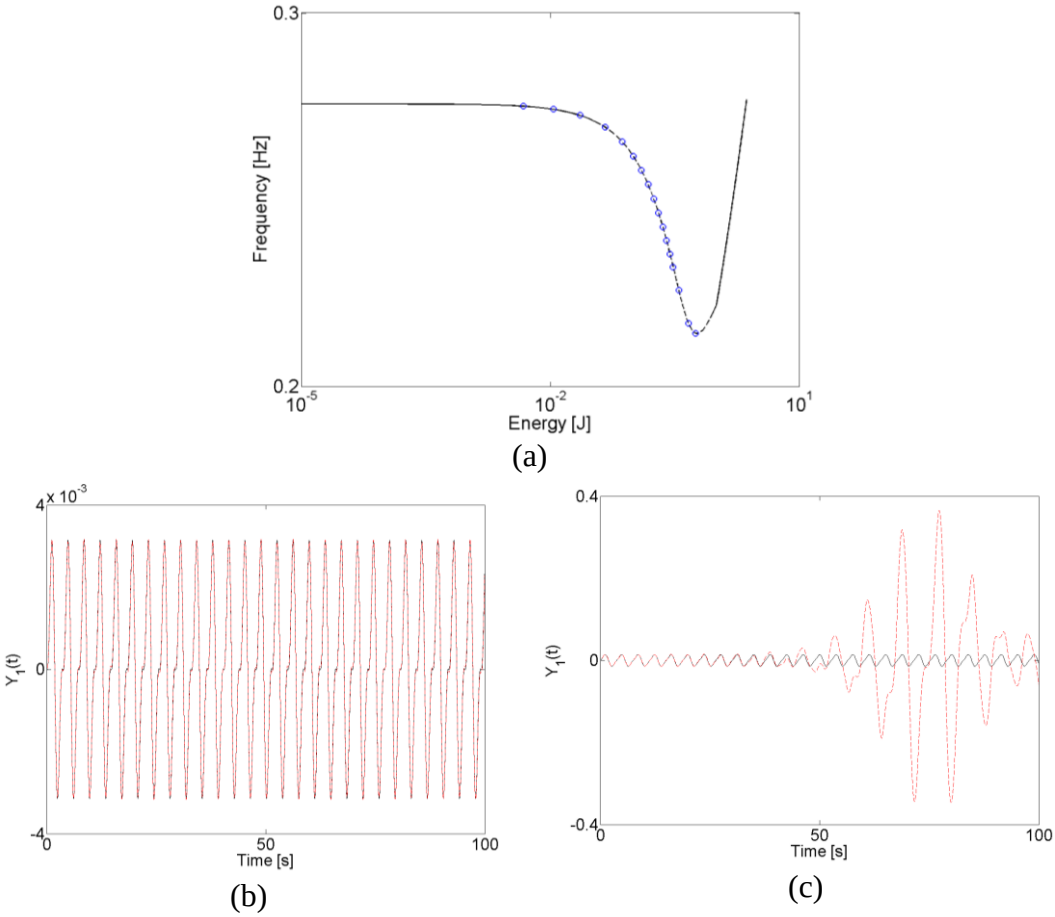

Figure 5. Second NNM. (a) Comparison between the frequency extracted from the invariant manifold (O) and the reference FEP from continuation. The dashed line corresponds to the unstable part of the backbone. (b-c) Slave velocity $\boldsymbol{Y_1}$ time series reduced on the manfold (black) and for the full-system (red). Perfect matcing for low amplitude initial conditions (b). Large discrepancies are observed after 40 seconds.

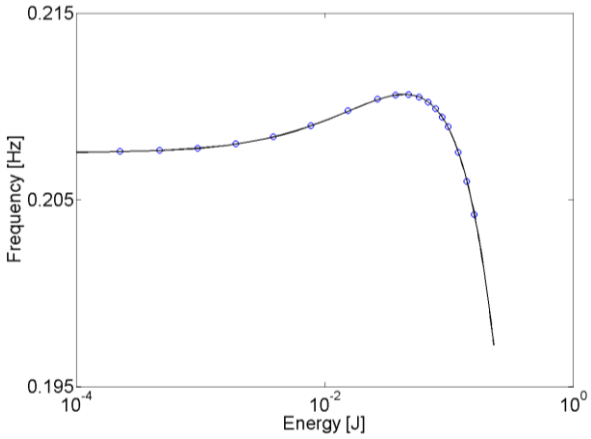

Figure 6. FEP for the first NNM with system parameters $\boldsymbol{\omega_1^2 = 1.7}$ and $\boldsymbol{\omega_2^2 = 6}$. Hardening behaviour turns to softening. Frequency extracted from the invariant manifold (O).

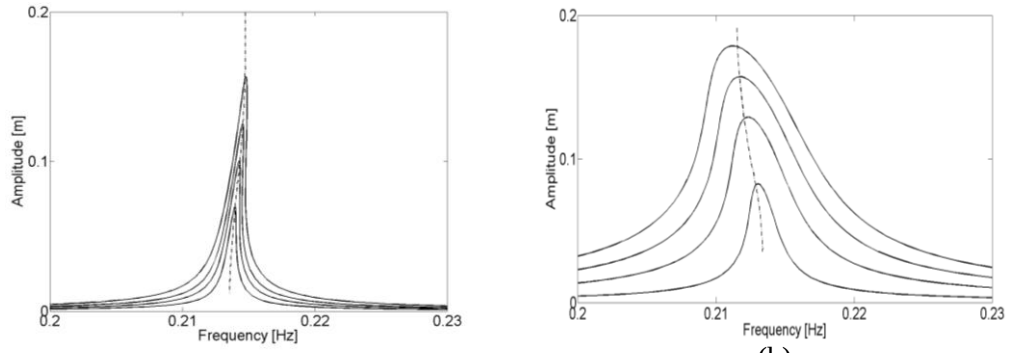

Figure 7. Frequency response curves to harmonic forcing. The hardening behaviour of the system at low linear damping (a) $(\boldsymbol{\xi_1}, \boldsymbol{\xi_2}) = (\mathbf{0.001}, \mathbf{0.005})$ turns to softening for higher damping values (b) $(\boldsymbol{\xi_1}, \boldsymbol{\xi_2}) = (\mathbf{0.001}, \mathbf{0.2})$. Frequency parameters are $\left(\boldsymbol{\omega_1^2}, \boldsymbol{\omega_2^2}\right) = (\mathbf{1.8}, \mathbf{6})$. The dashed-dot lines correspond to the NNM prediction using the invariant manifold approach. The frequency is computed by means of time integration and wavelet time-frequency analysis.

6. COUPLED VAN DER POL OSCILLATORS

A 2DOF example with nonlinear damping is now considered. It is a system of two coupled Van der Pol oscillators (cf. eq. (8)). System parameters are $c_{11} = c_{22} = 0$, $c_{12} = -c_{21} = 0.8$, $\epsilon_1 = \epsilon_2 = 0.5$, $\delta_1 = \delta_2 = 1$. We note here the presence of velocity dependent but however conservative terms ($c_{ji}x_i$). These terms have to be considered to properly fit iso-energy curves.

$$\begin{aligned} &\ddot{x}_1 + c_{11}\dot{x}_1 + c_{12}\dot{x}_2 - \epsilon_1(1 - x_1^2 - \delta_1 x_2^2)\dot{x}_1 + x_1 = 0 \\ &\ddot{x}_2 + c_{21}\dot{x}_1 + c_{22}\dot{x}_2 - \epsilon_2(1 - \delta_2 x_1^2 - x_2^2)\dot{x}_2 + 4x_2 = 0 \end{aligned} \tag{8}$$

Figure 8 presents the first invariant manifold computed starting from the first LNM. The slave DOFs are presented in Figure 8(a, b). The computation of the dynamics shows that a limit cycle is enclosed into the surface (Figure 8(c)). In the presence of damping, the validation of our results only relies of the accurate prediction of the dynamics. Figure 8(d) presents the time series of X_2 and compares it to the full-system dynamics. A perfect agreement is observed. To further validate this dynamics, a quantitative comparison is performed using the normalized mean square error (NMSE). In the present situation, the NMSE values reaches 1e-4% which is a sign of perfect matching.

7. CONCLUSIONS

In this paper, a novel method to solve NNMs as invariant manifold was presented. The key feature of the method is the interpretation of manifold governing PDEs as hyperbolic equations. These equations require specific numerical treatment in terms of discretization techniques as well as boundary conditions. The finite element method as the advantage to directly propose a way to compute the system reduced dynamics. Additional interpolations are not necessary. For conservative cases, a method proposed to retrieve the motion frequency as a byproduct of the invariant manifold computation. It is arguably the first method that addresses both conservative and nonconservative systems including linear as well as nonlinear damping.

Acknowledgements. The author L. Renson would like to acknowledge the Belgian National Fund for Scientific Research (FRIA fellowship) for its financial support.

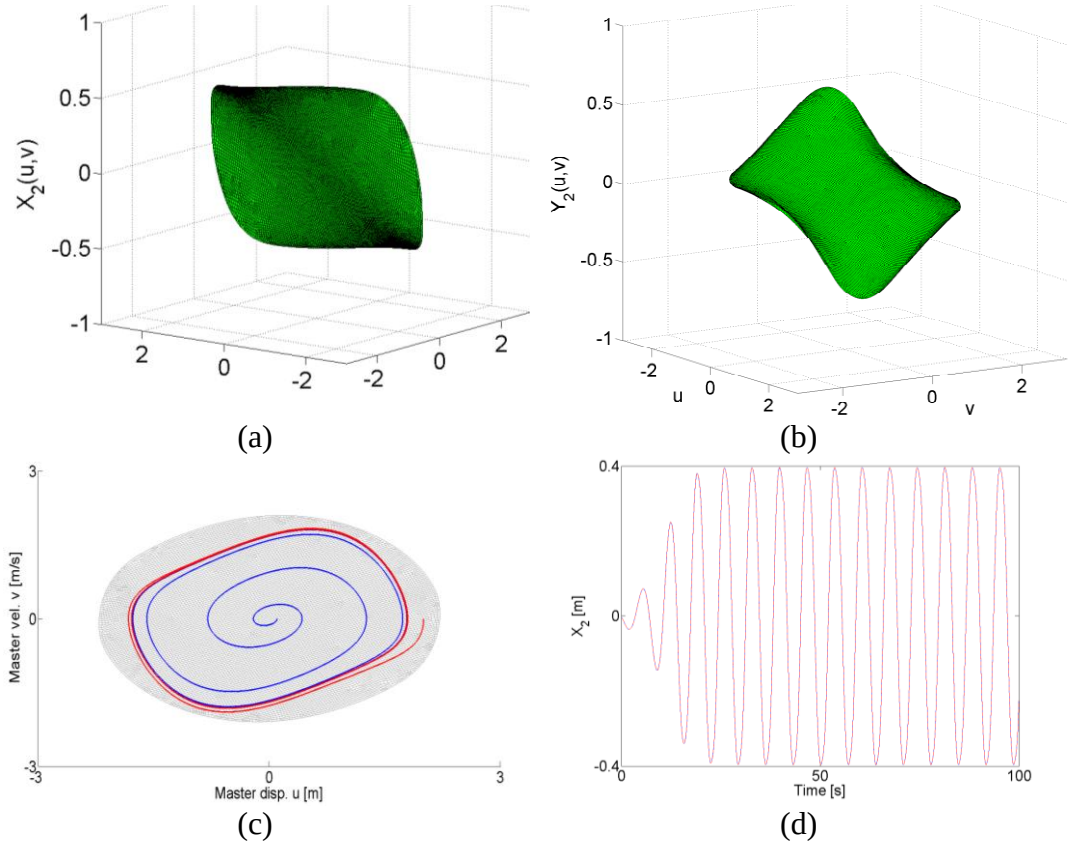

Figure 8. Invariant manifold computed from the first LNM. (a-b) Slave displacement $\boldsymbol{X_2}$ and velocity $\boldsymbol{Y_2}$. (c) The manifold encloses the limit cycle. (d) Slave displacement $\boldsymbol{X_2}$ dynamics versus time. The reduced dynamics perfectly reproduces the full-system dynmics. The NMSE equals $\boldsymbol{1e-4}$%.

REFERENCES

[1] Rosenberg, R. M. (1966). "On Nonlinear Vibrations of Systems with Many Degrees of Freedom." Advances in Applied Mechanics Volume 9: 155-242.

[2] Rosenberg, R. M. (1962). "The Normal Modes of Nonlinear n-Degree-of-Freedom Systems." Journal of Applied Mechanics 29(1): 7-14.

[3] Kerschen, G., M. Peeters, et al. (2009). "Nonlinear normal modes, Part I: A useful framework for the structural dynamicist." Mechanical Systems and Signal Processing 23(1): 170-194.

[4] Arquier, R., S. Bellizzi, et al. (2006). "Two methods for the computation of nonlinear modes of vibrating systems at large amplitudes." Computers & Structures 84(24-25): 1565-1576.

[5] Peeters, M., R. Viguié, et al. (2009). "Nonlinear normal modes, Part II: Toward a practical computation using numerical continuation techniques." Mechanical Systems and Signal Processing 23(1): 195-216.

[6] Shaw, S. W. and C. Pierre (1991). "Non-linear normal modes and invariant manifolds." Journal of Sound and Vibration 150(1): 170-173.

[7] Pesheck, E., C. Pierre, et al. (2002). "A New Galerkin-Based Approach for Accurate Non-Linear Normal Modes through Invariant Manifolds." Journal of Sound and Vibration 249(5): 971-993.
[8] Bellizzi, S. and R. Bouc (2005). "A new formulation for the existence and calculation of nonlinear normal modes." Journal of Sound and Vibration 287(3): 545-569.
[9] Bellizzi, S. and R. Bouc (2007). "An amplitude-phase formulation for nonlinear modes and limit cycles through invariant manifolds." Journal of Sound and Vibration 300(3-5): 896-915.
[10] Laxalde, D. and M. Legrand (2011). "Nonlinear modal analysis of mechanical systems with frictionless contact interfaces." Computational Mechanics 47(4): 469-478.
[11] Blanc, F., C. Touzé, et al. (2013). "On the numerical computation of nonlinear normal modes for reduced-order modelling of conservative vibratory systems." Mechanical Systems and Signal Processing 36(2): 520-539.
[12] Shaw, S. W. and C. Pierre (1993). "Normal modes for non-linear vibratory systems." Journal of Sound and Vibration 164: 40.
[13] Vakakis, A. F., L. I. Manevitch, et al. (2008). Frontmatter. Normal Modes and Localization in Nonlinear Systems, Wiley-VCH Verlag GmbH: I-XIII.
[14] Donea, J. and A. Huerta (2005). Steady Transport Problems, John Wiley & Sons, Ltd.
[15] Brooks, A. N. and T. J. R. Hughes (1982). "Streamline upwind/Petrov-Galerkin formulations for convection dominated flows with particular emphasis on the incompressible Navier-Stokes equations." Computer Methods in Applied Mechanics and Engineering 32(1–3): 199-259.
[16] Hughes, T. J. R. and T. E. Tezduyar (1984). "Finite element methods for first-order hyperbolic systems with particular emphasis on the compressible euler equations." Computer Methods in Applied Mechanics and Engineering 45(1–3): 217-284.
[17] Knobloch, Petr. "On the definition of the SUPG parameter." ETNA. Electronic Transactions on Numerical Analysis [electronic only] 32 (2008): 76-89.
[18] Tezduyar, T. E. and Y. Osawa (2000). "Finite element stabilization parameters computed from element matrices and vectors." Computer Methods in Applied Mechanics and Engineering 190(3–4): 411-430.
[19] Akin, J. E. and T. E. Tezduyar (2004). "Calculation of the advective limit of the SUPG stabilization parameter for linear and higher-order elements." Computer Methods in Applied Mechanics and Engineering 193(21–22): 1909-1922.
[20] Codina, R., E. Oñate, et al. (1992). "The intrinsic time for the streamline upwind/Petrov-Galerkin formulation using quadratic elements." Computer Methods in Applied Mechanics and Engineering 94(2): 239-262.
[21] Stein, K., T. E. Tezduyar, et al. (2004). "Automatic mesh update with the solid-extension mesh moving technique." Computer Methods in Applied Mechanics and Engineering 193(21–22): 2019-2032.
[22] Touzé, C. and M. Amabili (2006). "Nonlinear normal modes for damped geometrically nonlinear systems: Application to reduced-order modelling of harmonically forced structures." Journal of Sound and Vibration 298(4-5): 958-981.
[23] Touzé, C., O. Thomas, et al. (2004). "Hardening/softening behaviour in non-linear oscillations of structural systems using non-linear normal modes." Journal of Sound and Vibration 273(1-2): 77-101.